Strong and tunable couplings in flux-mediated optomechanics

Shevchuk, Olga; Steele, Gary A.; Blanter, Ya M.

DOI
10.1103/PhysRevB.96.014508

Publication date
2017

Document Version
Final published version

Published in
Physical Review B (Condensed Matter and Materials Physics)

Strong and tunable couplings in flux-mediated optomechanics

Olga Shevchuk, Gary A. Steele, and Ya. M. Blanter
Kavli Institute of Nanoscience, Delft University of Technology, Lorentzweg 1, 2628 CJ Delft, The Netherlands
(Received 21 November 2016; revised manuscript received 19 April 2017; published 11 July 2017)

We investigate a superconducting interference device (SQUID) with two asymmetric Josephson junctions coupled to a mechanical resonator embedded in the loop of the SQUID. We quantize this system in the case when the frequency of the mechanical resonator is much lower than the cavity frequency of the SQUID and in the case when they are comparable. In the first case, the radiation pressure and the cross-Kerr type interactions arise and are modified by the asymmetry. The cross-Kerr type coupling is the leading term at the extremum points where the radiation pressure is zero. In the second case, the main interaction is the single-photon beam splitter, which exists only at a finite asymmetry. Another interaction in this regime is of cross-Kerr type, which exists at all asymmetries, but is generally much weaker than the beam splitter interaction. Increasing magnetic field can substantially enhance the optomechanical couplings strength with a potential for the radiation pressure coupling to reach the single-photon strong coupling regime, even the ultrastrong coupling regime, in which the single-photon coupling rate exceeds the mechanical frequency.

DOI: 10.1103/PhysRevB.96.014508

I. INTRODUCTION

The progress in optomechanical systems, where optical or microwave cavities are coupled to mechanical resonators, has been impressive in recent years [1]. The accomplishments in optomechanics include cooling a mechanical resonator to its quantum ground state [2,3], prediction [4], and observation [5] of the optomechanically induced transparency, squeezing of the cavity [6,7] and the mechanical [8–10] modes, and coherent state transfer [11,12]. Many of these experiments have been realized using superconducting circuits, which enables us to view microwave cavities with mechanical elements as possible building blocks for quantum information processing [13].

The coupling between a cavity and a mechanical resonator plays a central role in optomechanics. In optomechanical systems, the origin of the coupling is the radiation pressure exerted by light on a mechanical resonator. This interaction is proportional to the number of photons in the cavity and thus is quadratic in the amplitude of the cavity field. It is also proportional to the mechanical displacement. In the published experiments, this intrinsically weak radiation pressure coupling was amplified by increasing the drive power of the cavity, which linearizes the effective optomechanical interaction of the system. This linearized interaction is known in optics as the beam splitter coupling. Such coupling would always turn Gaussian states of the cavity into Gaussian states of the mechanical resonator and vice versa. To create more general states for quantum information applications and to achieve, for instance, states with negative Wigner function, one needs to use either single-photon sources and photodetectors [14] or nonlinear effects, of which nonlinear optomechanical interaction is the most common one. The quantum effects in mechanical motion are thus best implemented in the so-called single-photon strong coupling regime, when the coupling strength exceeds the cavity decay rate [1]. In some configurations, the cavity is coupled to the position squared of the mechanical resonator [15], in which case strong coupling is needed as well. If, furthermore, the strength of the single-photon radiation pressure coupling can be made of the order of the mechanical frequency and larger than the cavity decay rate, the system is in the ultrastrong coupling regime, and photon blockade can be observed [16]. Single-photon strong coupling has never been achieved so far in optomechanical systems operating with optical light.

Along with ultracold atoms [17], superconducting circuits are promising candidates to reach strong and ultimately ultrastrong coupling. Recently, the idea of using the Josephson effect to enhance optomechanical couplings has been researched theoretically [18–21] and experimentally [22]. Many of those proposals involve using a superconducting quantum interference device (SQUID) with two Josephson junctions, which makes the cavity intrinsically nonlinear due to the Josephson effect. From the viewpoint of using optomechanical devices for quantum information transfer Josephson-based microwave optomechanical cavities thus have a double advantage: They provide additional nonlinearity to facilitate the creation of nonclassical states of a mechanical resonator, and the coupling between the cavity and the mechanical resonator can be strongly enhanced.

In this article, we concentrate on the form and the magnitude of optomechanical coupling. We consider a SQUID with two symmetric or asymmetric Josephson junctions and an embedded mechanical resonator and show that it by itself can produce ultrastrong optomechanical coupling. Originally, a dc SQUID with embedded mechanical oscillator was studied as a sensitive displacement detector [23–27]. It is well established that the coupling in such a SQUID cavity in the leading order is still the radiation pressure term, which depends on the applied flux and vanishes when the total flux through the SQUID equals to a half of the flux quantum Φ_0. For this value of the total flux, the next term, which is proportional to the numbers of both phonons and photons in the system, the so-called *cross-Kerr coupling*, becomes significant. However, the asymmetry of the junctions so far was not at the focus of attention of the literature, and theoretical proposals are routinely assuming that the two junctions of the SQUID are almost identical, whereas a certain asymmetry is always present in the experiment. We demonstrate that this asymmetry significantly affects the coupling strength and even leads in a new type of coupling not present in a symmetric SQUID cavity, *single-photon beam splitter coupling*, which becomes significant in the resonant

regime. In addition, we perform numerical simulations of the coupling rates for realistic experimental geometries. In doing so we find that this platform indeed has the potential to reach both the single-photon strong coupling, a regime of strong quadratic coupling of the motion to the cavity, and potentially the ultrastrong coupling regime where the single-photon coupling rate exceeds the mechanical frequency.

In the first part of the article, we investigate in details the effect of asymmetry in the SQUID with two junctions and embedded mechanical resonator. As a first step we look at the most common experimental situation of the mechanical frequency being much smaller than the cavity frequency [28]. We quantize the asymmetric system to obtain the radiation pressure interaction and the cross-Kerr type interaction, and to relate the coupling strengths to the parameters of the system. We show that for experimentally feasible parameters the radiation pressure coupling can reach single-photon strong coupling regime and for stronger magnetic fields even the ultrastrong coupling regime. The cross-Kerr coupling is usually much weaker than the radiation pressure coupling, but it is the leading coupling at the extremum points of the flux where the radiation pressure is zero. Such strong coupling could enable a quantum nondemolition measurement of a phonon number in the mechanical resonator [29] or the cavity's photon number.

As the second step, we study the case when the mechanical and cavity frequencies are of the same order. Since the SQUID cavity frequency is in the range of GHz, the same range would be required for the mechanical oscillator. Currently, carbon nanotube (CNT) resonators can reach GHz frequency [30] and, consequently, the realizations of the SQUID with suspended CNT junctions [31,32] could reach this regime. In this case, there are two leading interactions: the cross-Kerr and the single-photon beam splitter terms. The single-photon beam splitter exists only at the finite asymmetry. The radiation pressure term in this regime is oscillating too fast and can be, therefore, disregarded. In contrast to the standard optomechanical setups [1], where the beam splitter interaction is produced by the linearization of the radiation pressure term, in the SQUID cavity this is a separate term which is not related to the radiation pressure. The beam splitter is used in many experimental setups, and the Hamiltonian with the beam splitter interaction is easily diagonalized and solved. When the single-photon beam splitter term is in the strong coupling regime, one can observe, e.g., optomechanical normal-mode splitting [1]. The considerations and conclusions of this part also apply to the situation when the mechanical frequency is much lower than the SQUID cavity frequency, but the cavity is operated far from the resonance, at low frequencies, like it was the case with the dc experiments of Refs. [26–28].

The remainder of the article is organized as follows. In Sec. II we find the current and the cavity frequency of the SQUID with asymmetric Josephson junctions and an embedded mechanical resonator. In Sec. III we derive the effective Hamiltonian of this system for two cases. In the first case, the cavity frequency of the SQUID is taken to be much larger than the mechanical frequency, which results in the radiation pressure and the cross-Kerr interactions. In the second case, the cavity frequency is considered to be of the order of the mechanical frequency providing the single-photon beam splitter and the cross-Kerr interactions. In Sec. IV we draw the potential map and discuss optomechanical couplings. Finally, we provide the discussion of our results in Sec. V.

II. CURRENT OF THE ASYMMETRIC SQUID

In this section, we follow the standard textbook treatment of the current through an asymmetric SQUID, adding a coupled mechanical resonator. We consider two Josephson junctions with different values of critical current, I_1^0 and I_2^0, connected in a loop together with an embedded mechanical resonator, as shown in Fig. 1(a). The energy scales for such SQUID are described by the average Josephson energy $E_J = \hbar(I_1^0 + I_2^0)/4e$ and the charging energy $E_c = (2e)^2/2C \ll E_J$ with C being the shunting capacitance of each junction. The SQUID has a loop area A with the suspended arm of a length l. Oscillations of the mechanical resonator modulate the total flux of the SQUID loop. Then, the SQUID with the embedded mechanical resonator can be viewed as an LC circuit, in which the Josephson inductance of the SQUID L_J,

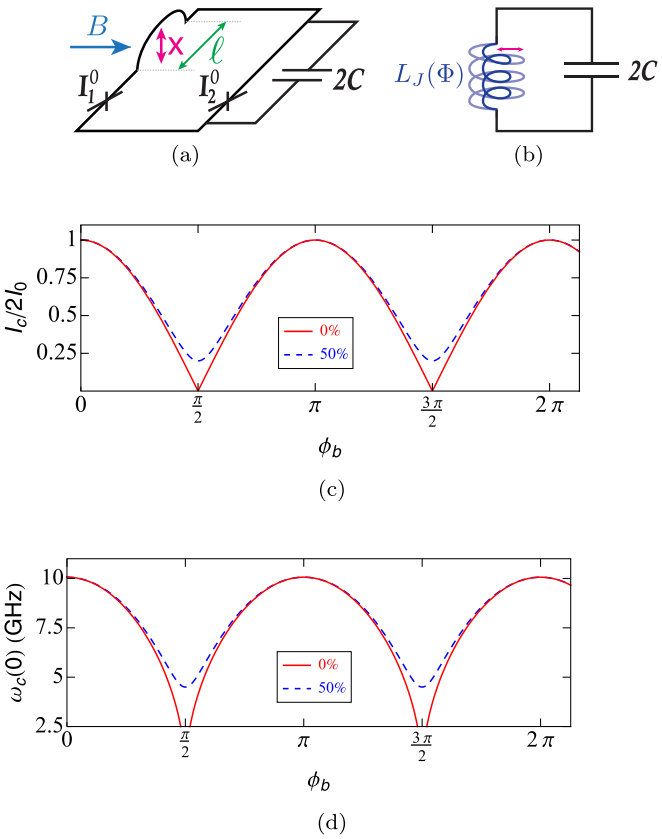

FIG. 1. (a) A schematic overview of the SQUID, which contains two Josephson junctions with different critical currents. The mechanical resonator is embedded into the SQUID loop. The magnetic field B is applied under certain angle to the loop, such the displacement X of the mechanical resonator results in a nonzero modulation of the magnetic flux through the loop. (b) The mechanical resonator couples inductively to the SQUID cavity via the total flux Φ. Here and below the color indicates the symmetry; 50% means $\alpha_I = 0.5$. (c) The critical current and (d) cavity frequency are plotted as a function of renormalized bias flux of the symmetric and asymmetric SQUID. The cavity frequency of the symmetric SQUID is cut at realistic value of 2.5 GHz.

which for symmetric junctions $I_1^0 = I_2^0 = I_0$ is well known to be $\Phi_0/[4\pi I_0 \cos(\pi\Phi/\Phi_0)]$, is modulated by the total flux Φ threading though the loop. Consequently, the cavity frequency is modulated by the flux, which results in the inductive coupling of the mechanical resonator and the SQUID, see Fig. 1(b). For simplicity, we assume that the mechanical resonator moves in its single mode. The dynamics of the mechanical resonator is described by the displacement X from its equilibrium position. The dynamics of the SQUID itself is described by the sum of the gauge-invariant phase differences across each junction (ϕ_1 and ϕ_2), $\varphi_+ = (\phi_1 + \phi_2)/2$, which is referred to as the overall phase of the SQUID. Moreover, the difference of the phases is bound by the total flux threading the loop

$$\varphi_- = (\phi_1 - \phi_2)/2 = \pi\Phi/\Phi_0 + \pi n\,, \tag{1}$$

where n is an integer and $\Phi_0 = h/2e$ is the flux quantum. Note that the value of n does not affect the results of the article.

Assuming the magnetic field is applied under certain angle to the SQUID loop the total flux can be separated to two contributions. The first contribution is the bias flux Φ_b, which is added to the SQUID loop in its fixed position, say for $X = 0$. The second contribution comes from the flux threaded the area swept by the oscillations of mechanical resonator. Since it is more convenient to work with the phase difference rather than the flux itself we define the renormalized bias flux $\phi_b = \pi\Phi_b/\Phi_0$ and renormalized flux shift provided by the resonator $\xi X = \pi\beta_0 BlX/\Phi_0$ with the average geometric constant β_0, which takes into account the direction of the magnetic field and the geometry of the mechanical resonator [26]. Then, the phase difference is given by

$$\varphi_- = \phi_b + \xi X + \pi n. \tag{2}$$

Here, we study the situation when the circuit has a negligible self-inductance.

Now we write the total current flowing through the asymmetric SQUID. For this purpose we introduce the average critical current $I_0 = (I_1^0 + I_2^0)/2$. The critical currents of the first and the second junctions are defined as $I_1^0 = I_0(1 - \alpha_I)$ and $I_2^0 = I_0(1 + \alpha_I)$, respectively, with the asymmetry parameter α_I. Therefore, the total current I through both junctions is separated into two terms: one is the same as in the case of equal critical currents and the second one, which is responsible for the influence of asymmetry

$$\begin{aligned} I &= I_1^0 \sin(\phi_1) + I_2^0 \sin(\phi_2) \\ &= 2I_0 \cos(\varphi_-)\sin(\varphi_+) - 2I_0\alpha_I \sin(\varphi_-)\cos(\varphi_+). \end{aligned} \tag{3}$$

To find the critical current of the asymmetric SQUID, we shift the position of the overall phase φ_+ of the SQUID by the phase φ_0 which satisfies the relation: $\tan(\varphi_0) = \alpha_I \tan(\varphi_-)$. Then, the total current is simplified to [33]

$$I = 2I_0 S(\varphi_-)\sin(\varphi_+ - \varphi_0), \tag{4}$$

where $S(\varphi_-) = \sqrt{\cos^2(\varphi_-) + \alpha_I^2 \sin^2(\varphi_-)}$ is a flux-dependent function, which turns to the absolute value of cosine at zero asymmetry, and the total current becomes the well-known expression for the symmetric SQUID. Then, when the mechanical resonator is at rest, we can define the maximum current and, hence, the critical current of the asymmetric SQUID as well as the cavity frequency

$$I(X = 0) = I_c = 2I_0 S_0 \quad \text{and} \quad \omega_c(0) = \sqrt{\frac{2\pi I_c}{C\Phi_0}}. \tag{5}$$

Here we use $S_0 = \sqrt{\cos^2(\phi_b) + \alpha_I^2 \sin^2(\phi_b)}$.

In Fig. 1(c) we show the behavior of the critical current for symmetric case ($\alpha_I = 0$) and for $\alpha_I = 0.5$. For identical junctions the current varies between 0 and $2I_0$, but in the presence of the asymmetry the current never reaches zero value. Even at the half flux quantum when the critical current for the symmetric case is zero, the critical current of the asymmetric SQUID is at minimum $I_c(\phi_b = \pi/2) = 2I_0\alpha_I$. Nevertheless, the maximum, which occurs at the odd integer flux quantum, is not affected by the asymmetry. The cavity frequency is proportional to $\sqrt{I_c}$ and portrays the same behavior of the critical current as shown in Fig. 1(d). For parameters of the critical current of the Josephson junction $I_0 = 500$ nA and capacitance $C = 30$ pF the maximum cavity frequency is 10 GHz. At half flux quantum and $\alpha_I = 0.5$, the cavity frequency reaches its minimum of 4.5 GHz.

III. QUANTIZATION

In the following, we quantize the system by starting with the classical Hamiltonian, which consists of the simple harmonic oscillator, kinetic energy, and the potential energy of the SQUID [34],

$$H = \frac{m_r \dot{X}^2}{2} + \frac{m_r \omega_m^2 X^2}{2} + \frac{C\Phi_0^2}{2(2\pi)^2}\dot{\varphi}_+^2 + E(\varphi_+, X), \tag{6}$$

where m_r and ω_m are the mass and the frequency of the mechanical resonator. The potential energy of the SQUID E is derived from the total current $\Phi_0 I/2\pi = \partial E/\partial\varphi_+$ found in Sec. II,

$$E(\varphi_+, X) = -2E_J S(\varphi_-)\cos[\varphi_+ - \arctan(\alpha_I|\tan\varphi_-|)]. \tag{7}$$

The minimum of the potential is shifted by a flux-dependent parameter, which also depends on the displacement of the mechanical resonator. Depending on the difference between the cavity frequency and the mechanical frequency one can assume quasistatic regime or has to take into account the displacement dependent shift.

A. Dispersive regime

In the typical case when the mechanical frequency is much smaller than cavity frequency, the shift by the flux can be assumed static on the timescales related to the SQUID. Then, we can write the potential energy in terms of the shifted phase $\varphi = \varphi_+ - \arctan(\alpha_I|\tan(\phi_b)|)$. The kinetic energy of the SQUID is not affected by the constant shift, and thus the phase φ_+ can be replaced by φ.

To quantize the phase and the position, the potential energy is expanded in terms of the phase up to the second order. This means that we consider SQUID as a linear harmonic oscillator, and the nonlinear effects are weak, having the amplitude smaller than the linewidth of the cavity and the cavity frequency. The term which is independent of the phase, shifts the equilibrium position of the mechanical resonator and

modifies the mechanical frequency

$$\omega_m' = \sqrt{\omega_m^2 + \frac{4E_J\xi^2\left(1-\alpha_I^2\right)\left[\cos^4(\phi_b) - \alpha_I^2\sin^4(\phi_b)\right]}{m_r S_0^3}}. \quad (8)$$

For the phase-dependent terms we introduce creation and annihilation operators

$$\begin{pmatrix} a^\dagger \\ a \end{pmatrix} = \frac{1}{\sqrt{2\hbar m_\varphi \omega_c}}(m_\varphi\omega_c\varphi \mp i p_\varphi), \quad (9)$$

with the momentum $p_\varphi = C\Phi_0^2/(2\pi)^2\dot{\varphi} \equiv m_\varphi\dot{\varphi}$, where m_φ is the mass of the phase, and the displacement dependent cavity frequency is

$$\omega_c(\varphi_-) = \sqrt{\frac{4\pi I_0 S(\varphi_-)}{C\Phi_0}}. \quad (10)$$

This expression can also be retrieved from Eq. (5) for the mechanical resonator at rest by changing ϕ_b to φ_-. Therefore, the displacement dependent cavity frequency as a function of φ_- has the same behavior as shown in Fig. 1(c).

Now our Hamiltonian has the form similar to that of the Hamiltonian with symmetric Josephson junctions except for the modified cavity frequency

$$H = \frac{m_r\dot{X}^2}{2} + \frac{m_r\omega_m^2 X^2}{2} + \hbar\omega_c(\varphi_-)a^\dagger a. \quad (11)$$

The position of the mechanical resonator is quantized by introducing the position operator, $X = x_{\rm ZPF}(b^\dagger + b)$, where b and $b^\dagger$ are creation and annihilation operators and $x_{\rm ZPF} = \sqrt{\hbar/2m_r\omega_m}$ is the amplitude of zero point fluctuations of the displacement X. Then, the uncoupled Hamiltonian of the mechanical resonator is $\hbar\omega_m b^\dagger b$.

The interaction terms are obtained by expanding the displacement dependent cavity frequency to the second order in displacement. Then, the interaction Hamiltonian after applying the rotation-wave approximation becomes

$$H_{int} = \hbar g_{RP}^1 a^\dagger a(b^\dagger + b) + \hbar g_Q^2 a^\dagger a b^\dagger b, \quad (12)$$

where the radiation pressure coupling and the cross-Kerr coupling between the cavity and the mechanical resonator are, respectively,

$$\begin{aligned} g_{RP}^1 &= x_{ZPF}\frac{\partial\omega_c}{\partial X}\bigg|_{X=0} = x_{ZPF}\xi\frac{\partial\omega_c}{\partial\varphi_-}\bigg|_{X=0} \\ &= x_{ZPF}\frac{\left(1-\alpha_I^2\right)\xi\sin(2\phi_b)\omega_c(0)}{4S_0^2}, \end{aligned} \quad (13)$$

$$\begin{aligned} g_Q^2 &= x_{ZPF}^2\frac{\partial^2\omega_c}{\partial X^2}\bigg|_{X=0} = x_{ZPF}^2\xi^2\frac{\partial^2\omega_c}{\partial\varphi_-^2}\bigg|_{X=0} \\ &= 2x_{ZPF}\xi g_{RP}^1\cot(2\phi_b) - \frac{3\left(g_{RP}^1\right)^2}{\omega_c(0)}. \end{aligned} \quad (14)$$

The first term is the usual radiation pressure interaction which is expected in an optomechanical cavity, where photons produce a force acting on a mechanical resonator. The only difference with our situation is that photons are in the microwave range. This term vanishes at $\phi_b = \pi/2$. The second term (cross-Kerr) is due to nonlinearity of the cavity and is normally much weaker than the radiation pressure. However, when $g_{RP}^1 = 0$, the first term in Eq. (14) stays finite because $\sin(2\phi_b)$ in the radiation pressure coupling is multiplied with the infinite factor $\cot(2\phi_b)$. Thus, close to $\phi_b = \pi/2$, the cross-Kerr term can become dominant.

Let us now briefly discuss the physical interpretation of Eq. (12). We note that Josephson effect is not essential for creation of the force. For example, if we have a microwave LC circuit, which in its simplest realization is a loop threaded by magnetic flux and capacitively coupled to a nearby electrode, it has the inductive energy, LI^2, where L is the inductance of the loop, and I is the current through the loop. The inductance depends on the geometric size of the loop, and thus, if the loop is deformed by mechanical motion, e.g., if its part is suspended, the inductive energy depends on the position x of the mechanical resonator embedded in the loop, thereby providing a mechanical force. This force is $F = -(dL/dx)I^2$, dL/dx can be approximated by a constant, and after quantization of the current the interaction becomes formally of the same functional form as the radiation pressure force. For a SQUID loop, physics is the same, however, the inductive-like energy is stored in the Josephson junctions, and the coupling is much stronger and oscillates strongly as a function of the external magnetic field. Furthermore, at certain values of the flux the coupling, proportional to dL/dx, vanishes, and one needs to expand the inductance to the order x^2. This procedure provides the cross-Kerr coupling.

To visualize the resulting couplings, to the chosen capacitance C and critical current I_0 we add the following set of parameters: $\omega_m' = 10$ MHz, $A = 200\ \mu\text{m} \times 150\ \mu\text{m}$, $l = 150\ \mu$m, and $m_r = 200$ pg. The flux bias varies from $\phi_b = 2\pi n$ to $\phi_b = 2\pi n + \pi$, where $n = 72534$ corresponds to chosen value of magnetic field.

In Fig. 2(a), we plot the radiation pressure coupling. For the perfectly symmetric Josephson junctions, the absolute value of the radiation pressure infinitely increases while getting closer to the half-integer flux quantum. It suggests that if in the experiment one can tune bias flux very close to the half flux quantum the radiation pressure will be maximum. However, because of the asymmetry of the SQUID the maximum of the radiation pressure coupling shifts to the value of the flux given by $\tan(\phi_b) = \pm\sqrt{1-\alpha_I^2+\sqrt{1+14\alpha_I^2+\alpha_I^4}}/2\alpha_I$. Beyond this value, the radiation pressure monotonically decreases to zero at the half-integer flux quantum. The maximum of the radiation pressure even at $\alpha_I = 0.5$ and magnetic field of 10 mT can reach single-photon strong coupling regime, considering a typical cavity decay rate of 80 kHz.

The divergence of the radiation pressure coupling, here and below, for a symmetric SQUID ($\alpha_I = 0$) in the limit of $\phi_b = \pi/2$ is due to the behavior of the cavity frequency as $\omega_c(\varphi_-) \propto |\cos\varphi_-|^{1/2}$. However, our treatment is not valid strictly in this limit since it is based on the assumption that the cavity frequency shift is small compared to the cavity frequency itself. If a symmetric SQUID is biased exactly at $\phi_b = \pi/2$, due to the mechanical motion the phase ϕ_- oscillates between $\pi/2 \pm \xi X$, and the divergences will be smeared for $\pi/2 - \xi X < \phi_b < \pi/2 + \xi X$. To consider this regime, one needs to go beyond the Taylor expansion of the cavity frequency. In addition, close to $\phi_b = \pi/2$ the cavity, even in the asymmetric case, can not be considered as linear. This also creates a limitation on how close

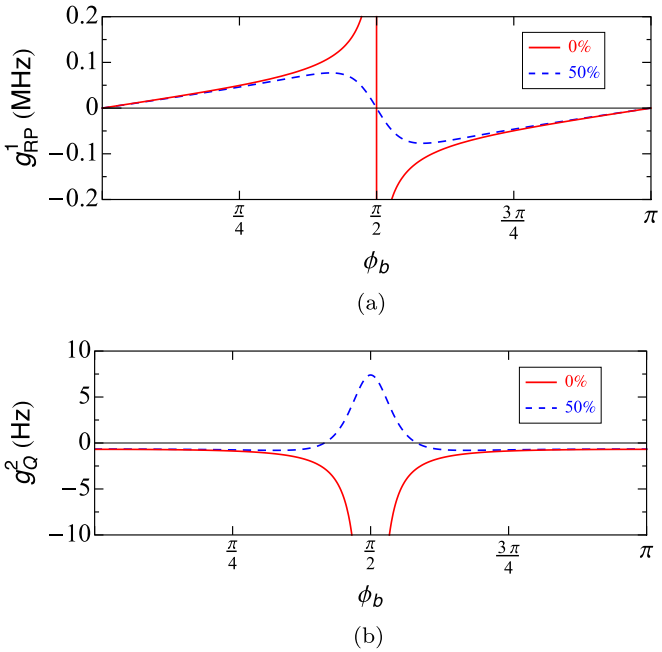

FIG. 2. Light-matter couplings of symmetric and asymmetric SQUID for magnetic field $B = 10$ mT: (a) radiation pressure, (b) cross-Kerr coupling. The maximum of radiation pressure for $\alpha_I = 0.5$ is $g^1_{RP} = 77$ kHz. The flux bias is shifted by $\pi BA/\Phi_0 = 2\pi 72534$. We see that the radiation pressure coupling diverges at $\alpha_I = 0$ and $\phi_b = \pi/2$; this divergence is in reality smeared as discussed in the text.

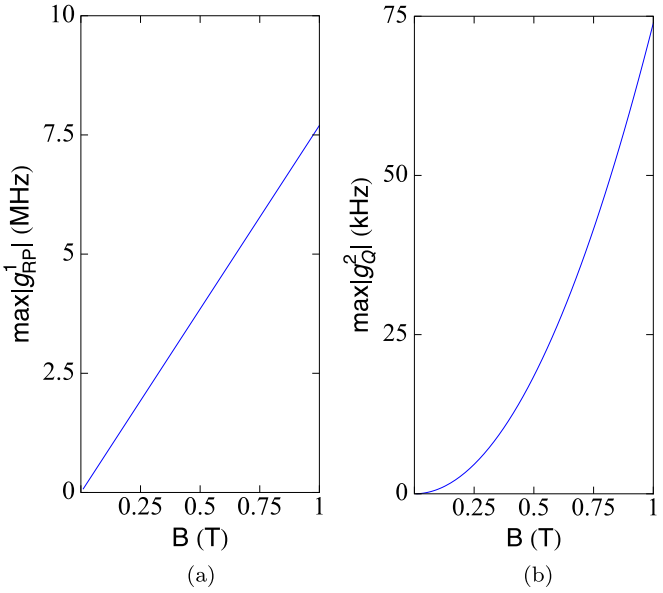

FIG. 3. The maximum value of the (a) radiation pressure and (b) cross-Kerr coupling as a function of the magnetic field at $\alpha_I = 0.5$. The flux bias is fixed and corresponds to the sweet spot (maximum) of each coupling, respectively. The field dependence is linear in (a) and quadratic in (b), and thus both couplings can be significantly enhanced by magnetic field. For our chosen parameters, at 1 T the radiation pressure coupling becomes comparable with the mechanical frequency.

we can approach this bias point. We discuss this limitation in Sec. IV.

Since the radiation pressure can also be written in terms of the cavity frequency derivative, we can analyze this coupling looking at Fig. 1(c) by changing ϕ_b to φ_- as mentioned above. For the asymmetric case the slope of the frequency increases and then decreases while varying the flux from 0 to $\pi/2$. After crossing $\pi/2$ to π it changes the sign of the slope, which leads to the negative radiation pressure. Also, for asymmetric junctions the slope at the integer and the half-integer flux quantum is zero.

The cross-Kerr coupling is shown in Fig. 2(b). For the symmetric case the coupling is infinitely strong approaching the half-integer flux quantum, which is the same behavior as found for the radiation pressure, but in contrast to the latter it does not change the sign while crossing $\pi/2$. Looking at Fig. 1(c) we expect that for the asymmetric SQUID the cross-Kerr coupling, which is the second derivative of the cavity frequency over the displacement, changes the sign between 0 to $\pi/2$ and then from $\pi/2$ to π and this is indeed the result observed here. The maximum of the coupling for the asymmetric case is achieved at the half-integer flux quantum. We also notice that even at the flux equal to the integer number of flux quanta the value of the cross-Kerr coupling (for the chosen parameters) is 0.66 Hz. In the experiment with the membrane inside the cavity [15] the value of the second derivative of the cavity frequency was $\omega_c''(x)/2\pi = 108$ kHz nm^{-2}. Then to improve this value multiple modes of the cavity were coupled to the single mode of the mechanical resonator [35] to get $\omega_c''(x)/2\pi = 8.7$ MHz nm^{-2}, which is still lower than our calculated value at the flux equal to the integer number of flux quanta, which is $\omega_c''(x)/2\pi = 4$ GHz nm^{-2}.

The maximum value of the asymmetric couplings increases with magnetic field, as shown in Fig. 3. Increasing magnetic field to 1 T is experimentally feasible [32] and increases chances of getting stronger couplings. The radiation pressure coupling is linearly dependent on B and the cross-Kerr coupling is quadratically dependent on B. At $\alpha_I = 0.5$ and magnetic field of 1 T the radiation pressure can reach the ulrastrong coupling regime ($g^1_{RP} \sim \omega_m$), which also means that at lower asymmetry the value on the sweet spot can even be greater. The cross-Kerr coupling can reach values of 80 kHz. It can be stronger for the lower asymmetry, but the window to catch the sweet spot becomes more narrow for the lower asymmetry.

B. Resonant frequencies

Here, we consider the regime in which the mechanical resonator and the cavity operate at comparable frequencies. This is relevant for the case when the mechanical frequency and the cavity frequency have the same order, and also for the case when the cavity frequency operates in the dc regime or far off resonance, like it was in the experiments Refs. [26–28].

Now, the minimum of the potential is shifted by a position-dependent parameter, see Eq. (7). However, the displacement is now one of the dynamical variables of the system, separate from the overall phase. If we shift the phase by a displacement-dependent parameter then the kinetic energy acquires the

shifted phase as well as extra terms in the form of $\dot{\varphi}_+\dot{X}$ with the original phase. Therefore, it is simpler to expand the arctangent in the potential energy to the first order in X, which is sufficient since the amplitude of the mechanical resonator is usually small in such devices. The expanded potential energy depends on both the displacement and the phase φ, which do not combine into a single variable

$$E(\varphi,X) = -2E_J S(\varphi_-)\cos\left(\frac{\alpha_I\xi}{S_0^2}X\right) - 2E_J S(\varphi_-)\sin\left(\frac{\alpha_I\xi}{S_0^2}X\right)\varphi + E_J S(\varphi_-)\cos\left(\frac{\alpha_I\xi}{S_0^2}X\right)\varphi^2. \quad (15)$$

Similarly to the previous case, the first term shifts the equilibrium position of the mechanical resonator and the mechanical frequency

$$\omega_m' = \sqrt{\omega_m^2 + \frac{2E_J\xi^2\sqrt{2\left[1+\alpha_I^2+\left(1-\alpha_I^2\right)\cos(2\phi_b)\right]}}{m_r}}. \quad (16)$$

Next, we quantize the phase introducing the operators $a^\dagger$, a. The momentum variable $p_\varphi = m_\varphi\dot{\varphi}$ stays the same as in the previous case, however, the displacement-dependent cavity frequency is different from Eq. (10),

$$\omega_c(X) = \sqrt{\frac{4\pi I_0 S(\varphi_-)\cos\left(\frac{\alpha_I\xi}{S_0^2}X\right)}{C\Phi_0}}. \quad (17)$$

Then, the Hamiltonian in terms of the cavity operators has the following form:

$$H = \frac{m_r\dot{X}^2}{2} + \frac{m_r{\omega_m'}^2X^2}{2} + \hbar\omega_c(X)a^\dagger a, \quad (18)$$

$$- \frac{2\hbar I_0 S(\varphi_-)}{\sqrt{2\hbar C\omega_c(X)}}\sin\left(\frac{\alpha_I\xi}{S_0^2}X\right)(a^\dagger + a). \quad (19)$$

We expand the full Hamiltonian to the second order in the displacement and use the creation and annihilation operators $b^\dagger$, b of the mechanical resonator. This procedure yields the uncoupled cavity Hamiltonian $\hbar\omega_c(0)a^\dagger a$ and the uncoupled mechanical resonator Hamiltonian $\hbar\omega_m' b^\dagger b$. Applying the rotating-wave approximation results in the interaction Hamiltonian of the following form:

$$H_{int} = \hbar g_Q^{2r} a^\dagger a b^\dagger b - \hbar g_{BS}^{1r}(a^\dagger b + b^\dagger a), \quad (20)$$

where the cross-Kerr and the single-photon beam splitter couplings, respectively, are

$$g_Q^{2r} = x_{ZPF}^2\frac{\partial^2\omega_c^r}{\partial X^2}\bigg|_{X=0} = g_Q^2 - \frac{\alpha_I^2\xi^2}{2S_0^4}\omega_c(0), \quad (21)$$

$$g_{BS}^{1r} = x_{ZPF}\frac{\alpha_I\xi\sqrt{\omega_c(0)E_J}}{\sqrt{\hbar S_0^3}}. \quad (22)$$

The cross-Kerr coupling has the same meaning as in the dispersive regime, Eq. (12). However, instead of the radiation pressure coupling present in Eq. (12) we have now the linear beam splitter coupling. Note that it is remarkably different from the standard optomechanics case [1]. In optomechanics, the beam-splitter coupling is obtained by linearization of the radiation pressure coupling at large number of photons in the cavity N, is enhanced by the factor of $\sqrt{N}$, and is therefore referred to as multiphoton beam-splitter coupling. In contrast, in our case the beam-splitter coupling naturally appears in the Hamiltonian and does not contain $\sqrt{N}$ as a prefactor, therefore it is single-photon beam-splitter coupling. The origin of this coupling is the Lorentz force [28]. Since we have charges moving in the external magnetic field, the mechanical Lorentz force acting on a suspended junction is proportional to the current through the junction, and the current is proportional to the superconducting phase at low phase differences, which gives Eq. (20).

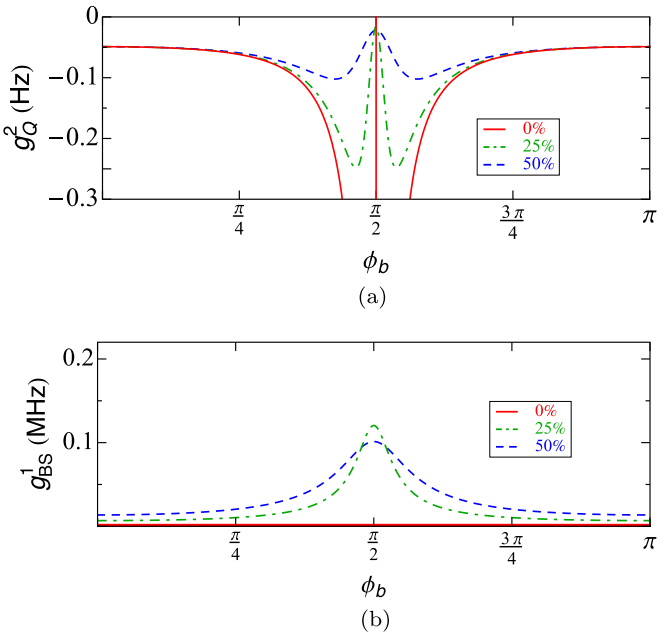

FIG. 4. Interaction couplings for symmetric and asymmetric SQUID in the case of $\omega_c(0) \sim \omega_m'$ and magnetic field $B = 10$ mT: (a) cross-Kerr coupling, (b) single-photon beam splitter coupling. The flux bias is shifted by $12\pi BA/\Phi_0 = 2\pi\cdot 18$. Similarly to the dispersive case, the cross-Kerr coupling diverges close to $\phi_b = \pi/2$ for a symmetric SQUID cavity. This divergence is cutoff in the same manner as we discussed for the dispersive regime. In contrast, the single-photon beam splitter coupling is finite and vanishes for a symmetric SQUID cavity.

To plot these couplings, we use the following set of parameters for the nanoSQUID with CNT junctions [31]: $I_0 = 15$ nA, $C = 90$pF, $A = 800$ nm $\times$ 800 nm, $l = 200$ nm, and $m_r = 5$ ag. The cavity frequency for these values is 1 GHz. The mechanical frequency is taken to be $\omega_m' = 1$ GHz, which is possible to reach with a suspended CNT. The flux bias varies from $\phi_b = 2\pi n$ to $\phi_b = 2\pi n + \pi$, where $n = 18$.

In Fig. 4(a), we plot the cross-Kerr coupling as a function of the magnetic flux. The coupling g_Q^2 is overall weaker than the one we found in Fig. 2(b). For the symmetric case, the behavior is the same as we have seen in the dispersive regime. However, for finite asymmetry the behavior is qualitatively

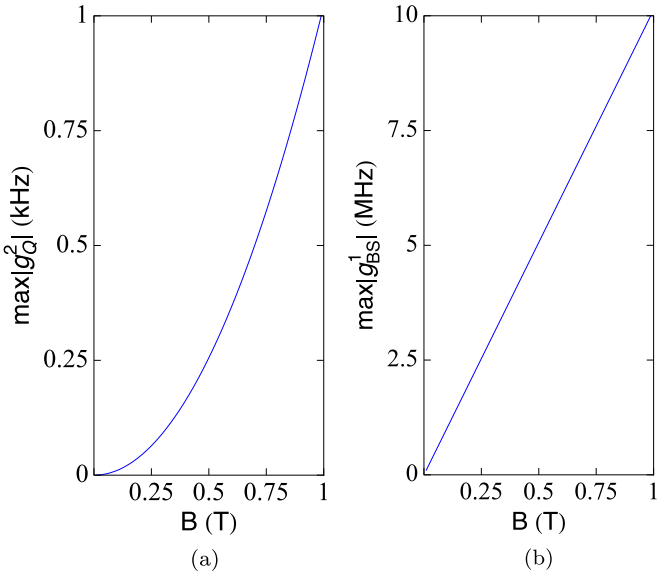

FIG. 5. The maximum of (a) the cross-Kerr coupling and (b) the single-photon beam splitter coupling at $\alpha_I = 0.5$ as a function of the magnetic field corresponding to Fig. 4. The flux bias is fixed to the sweet spot of each coupling. Similarly to the dispersive case, the beam splitter coupling is linear in magnetic field, whereas the cross-Ker coupling is quadratic.

different since the coupling is negative and does not change sign from negative to positive. Also, there is a peak in the coupling close to $\pi/2$ and at exactly the half flux quantum there is a minimum. This happens because of the second term in Eq. (21), which arises due to the modified cavity frequency. For lower asymmetry the minimum is getting closer to zero while the maximum is increasing.

Figure 4(b) shows the single-photon beam splitter coupling. For $\omega_c(0) \gg \omega_m'$ this coupling is negligible because the corresponding term in the Hamiltonian is a quickly oscillating function of time. In or near the resonant regime, this coupling is significant but only exists at a finite asymmetry. The single-photon beam splitter coupling is slowly increasing while the flux rises from 0 to $\pi/2$ and reaches its maximum at the half flux quantum and then passing this point decreases again. For a lower asymmetry the peak is higher, but the window to reach higher value is narrower, since the higher asymmetry corresponds to a higher value of the coupling except for close to half-integer flux quantum.

In Fig. 5 we show the maximum value of both couplings at $\alpha_I = 0.5$ while increasing magnetic field to 1 T. The cross-Kerr coupling for our chosen parameters reaches 1 kHz, while the single-photon beam splitter coupling has the value of up to 10 MHz. This means that both couplings stay well below the mechanical frequency, so that the ultrastrong coupling regime is not reached, but depending on the cavity decay rate it can operate in the strong-coupling regime. Note again that g_{BS}^{2r} has intrinsically a beam splitter character even at the single-photon level, and does not originate from linearization of the radiation pressure coupling. At very low asymmetry and strong magnetic fields the cross-Kerr coupling can be larger than beam-splitter interaction.

IV. DISCUSSION

To gain an intuition about the couplings and to better understand the role of the asymmetry we plot the potential energy of the SQUID cavity as a function of flux (φ_-) and phase (φ_+) in Fig. 6. For the symmetric junctions the potential is symmetric along the dashed line. At the bottom of the potential, the radiation pressure is zero, and the cross-Kerr coupling is finite. For the asymmetric case, the potential has an elliptical form and is asymmetric. One can further study the figures on the bottom corresponding to the cross-section of the energy map for different flux. The cross-sections are chosen by moving the horizontal dashed line up. In the symmetric case the minimum of the potential energy always stays at the same position. In contrast, for the asymmetric junctions the position of the minimum shifts, which is also described by Eq. (7). In the case of dispersive frequencies, this shift is constant, and the minimum is redefined at each bias flux, which represents the same physics as for the symmetric case. However, the elliptical form alters the radiation pressure and the cross-Kerr couplings and changes their dependence of magnetic flux as previously appeared in Fig. 2 around half-integer flux quantum where there is a merge between elliptical forms.

For the case of resonant frequencies and an asymmetric SQUID, the minimum of the potential energy is shifted by the displacement dependent flux. The oscillations of the mechanical resonator correspond to the motion from one curve in Fig. 6 to another one. The force that triggers the motion between the minima of these curves is just like the Lorentz force, which explains the appearance of the single-photon beam splitter and the extra term picked up by cross-Kerr coupling as compared to the dispersive regime.

We now discuss the mechanical frequency shifts due to the Josephson term in Eqs. (8) and (16). In the parameter regime we have chosen this shift can be disregarded. However,

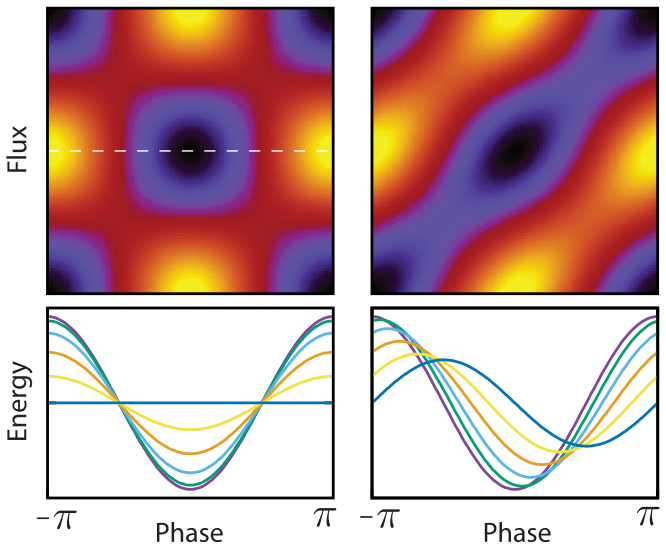

FIG. 6. Potential energy of the SQUID cavity as a function of the phase and flux at $\alpha_I = 0$ (left) and $\alpha_I = 0.5$ (right). The minimum is shown in black and maximum in yellow. The corresponding cross sections of energy map for the different values of the flux are displayed on the bottom. See the text for the discussion.

for higher values of Josephson energy increasing magnetic field to 1 T can create a large shift, which should be taken into account. The mechanical zero-point fluctuation in such a situation becomes smaller, subsequently the values of the couplings decrease, but we do not expect the change in the overall behavior of the optomechanical couplings.

Generally, the SQUID is an intrinsically nonlinear cavity. Close to the half-integer flux quantum, an extra nonlinear Kerr-type term $\Lambda a^\dagger a a a^\dagger$ appears in the Hamiltonian of Eqs. (11) and (19), where the Kerr nonlinearity is $\Lambda = \hbar\pi^2/(4C\Phi_0^2)$. This term results from the expansion of the potential energy to the fourth order in the overall phase φ. Thus, a cavity can be considered linear as long as Λ is less than the cavity linewidth and $\omega_c(0) \gg \Lambda$, which gives a finite condition for the flux bias close to the half integer flux quantum. Close to the half flux quantum the Kerr-type term and the cross-Kerr term are always present in this system. From the fourth-order expansion of the potential energy there are also other nonlinear interaction terms such as $a^\dagger a^\dagger a a b^\dagger b$ in the dispersive case or $a^\dagger a^\dagger a b$ in the resonant case, which are always small.

V. CONCLUSION

We provided a quantum analysis of the SQUID with asymmetric Josephson junctions and embedded mechanical resonator for the two cases of dispersive and resonant regimes of cavity and mechanical frequencies. We demonstrated that such a SQUID acts as an optomechanical microwave cavity. Our findings are relevant for the experimental setup where asymmetry cannot be avoided. For dispersive coupling, where the mechanical frequency is much lower than the SQUID cavity frequency, and the cavity is operated close to the resonance, we found that the radiation pressure coupling of the type $a^\dagger a(b^\dagger + b)$ dominates. However, in contrast to standard optomechanical cavities, the coupling strength depends on the magnetic flux through the SQUID. In a symmetric cavity, the coupling is the strongest close to the point where the half flux quantum is applied to the cavity, however, for any asymmetry the coupling vanishes exactly at this point. Away from this point, the coupling is really strong, even at $\alpha_I = 0.5$ and weak magnetic field, and the amplitude is proportional to the applied magnetic field. For high magnetic fields, the ultrastrong coupling regime of the radiation pressure can be achieved, which is currently a great challenge in cavity optomechanics. There is also the cross-Kerr coupling, $a^\dagger a b^\dagger b$, originating from the nonlinearity of the SQUID cavity. This coupling is much weaker than the radiation pressure, but at the half flux quantum it becomes the dominant coupling term since the radiation pressure amplitude is zero. For the symmetric case, the cross-Kerr coupling is always negative. For the asymmetric case, the cross-Kerr coupling has maximum at the half-integer flux quantum and changes sign from negative to positive while reaching a maximum.

In the resonant case, when the SQUID cavity is operated at low frequencies, compared to the mechanical frequency, we find qualitatively different results—the radiation pressure coupling does not play any role since it oscillates with a high frequency, and the dominant coupling term is the single-photon beam-splitter interaction $ab^\dagger + a^\dagger b$. This coupling is absent in the symmetric case at any magnetic field. The maximum of the beam-splitter coupling strength is at the half flux quantum. The cross-Kerr coupling is present as well but never dominates except for an ideally symmetric SQUID, $\alpha_I = 0$.

We explained the origin of different couplings using the potential energy map as well as compared the maps for the symmetric and the asymmetric cases. Concerning the strong radiation-pressure coupling in the dispersive regime, we expect it to be possible to realize with existing experimental parameters. The biggest challenge to experimentally realize the strong single-photon beam splitter coupling is the condition on the mechanical frequency, which should be comparable to the cavity frequency. It does not look realistic with existing setup, though using carbon nanotubes as a mechanical resonator coupled to the Josephson circuit one can potentially solve the high mechanical frequency issue. The workaround is to operate a SQUID cavity at low frequencies, resonantly with the mechanical resonator, such as it was done in Refs. [26–28].

Achieving strong or ultrastrong radiation pressure coupling would enable the SQUID-based optomechanics to perform experiments which are currently much sought by but not yet available for cavity optomechanics, mainly on quantum control of states of mechanical resonator and using it as a quantum transducer between different quantum media, for example, between optical and microwave light.

ACKNOWLEDGMENTS

This work was supported by the Netherlands Foundation for Fundamental Research on Matter (NWO-FOM).

[1] M. Aspelmeyer, T. J. Kippenberg, and F. Marquardt, Rev. Mod. Phys. **86**, 1391 (2014).
[2] J. Chan, T. P. M. Alegre, A. H. Safavi-Naeini, J. T. Hill, A. Krause, S. Gröblacher, M. Aspelmeyer, and O. Painter, Nature (London) **478**, 89 (2011).
[3] J. D. Teufel, T. Donner, D. Li, J. W. Harlow, M. S. Allman, K. Cicak, A. J. Sirois, J. D. Whittaker, K. W. Lehnert, and R. W. Simmonds, Nature (London) **475**, 359 (2011).
[4] G. S. Agarwal and S. Huang, Phys. Rev. A **81**, 041803 (2010).
[5] S. Weis, R. Rivire, S. Delglise, E. Gavartin, O. Arcizet, A. Schliesser, and T. J. Kippenberg, Science **330**, 1520 (2010).
[6] A. H. Safavi-Naeini, S. Gröblacher, J. T. Hill, J. Chan, M. Aspelmeyer, and O. Painter, Nature (London) **500**, 185 (2013).
[7] T. P. Purdy, P.-L. Yu, R. W. Peterson, N. S. Kampel, and C. A. Regal, Phys. Rev. X **3**, 031012 (2013).
[8] E. E. Wollman, C. Lei, A. Weinstein, J. Suh, A. Kronwald, F. Marquardt, A. Clerk, and K. Schwab, Science **349**, 952 (2015).
[9] F. Lecocq, J. B. Clark, R. W. Simmonds, J. Aumentado, and J. D. Teufel, Phys. Rev. X **5**, 041037 (2015).
[10] J.-M. Pirkkalainen, E. Damskägg, M. Brandt, F. Massel, and M. A. Sillanpää, Phys. Rev. Lett. **115**, 243601 (2015).

[11] V. Fiore, Y. Yang, M. C. Kuzyk, R. Barbour, L. Tian, and H. Wang, Phys. Rev. Lett. **107**, 133601 (2011).
[12] T. A. Palomaki, J. W. Harlow, J. D. Teufel, R. W. Simmonds, and K. W. Lehnert, Nature (London) **495**, 210 (2013).
[13] M. Wallquist, K. Hammerer, P. Rabl, M. Lukin, and P. Zoller, Phys. Scr. **T137**, 014001 (2009).
[14] E. Knill, R. Laflamme, and G. J. Milburn, Nature (London) **409**, 46 (2001).
[15] C. H. Bui, J. Zheng, S. W. Hoch, L. Y. T. Lee, J. G. E. Harris, and C. W. Wong, App. Phys. Lett. **100**, 021110 (2012).
[16] P. Rabl, Phys. Rev. Lett. **107**, 063601 (2011).
[17] S. Gupta, K. L. Moore, K. W. Murch, and D. M. Stamper-Kurn, Phys. Rev. Lett. **99**, 213601 (2007).
[18] J. R. Johansson, G. Johansson, and F. Nori, Phys. Rev. A **90**, 053833 (2014).
[19] T. T. Heikkilä, F. Massel, J. Tuorila, R. Khan, and M. A. Sillanpää, Phys. Rev. Lett. **112**, 203603 (2014).
[20] P. D. Nation, J. Suh, and M. P. Blencowe, Phys. Rev. A **93**, 022510 (2016).
[21] M. Abdi, M. Pernpeintner, R. Gross, H. Huebl, and M. J. Hartmann, Phys. Rev. Lett. **114**, 173602 (2015).
[22] J.-M. Pirkkalainen, S. U. Cho, F. Massel, J. Tuorila, T. T. Heikkilä, P. J. Hakonen, and M. A. Sillanpää, Nat. Commun. **6**, 6981 (2015).
[23] X. Zhou and A. Mizel, Phys. Rev. Lett. **97**, 267201 (2006).
[24] E. Buks and M. P. Blencowe, Phys. Rev. B **74**, 174504 (2006).
[25] S. Pugnetti, Y. M. Blanter, and R. Fazio, Europhys. Lett. **90**, 48007 (2010).
[26] S. Etaki, M. Poot, I. Mahboob, K. Onomitsu, H. Yamaguchi, and H. S. J. van der Zant, Nat. Phys. **4**, 785 (2008).
[27] S. Etaki, F. Konschelle, Ya. M. Blanter, H. Yamaguchi, and H. S. J. van der Zant, Nat. Commun. **4**, 1803 (2013).
[28] M. Poot, S. Etaki, I. Mahboob, K. Onomitsu, H. Yamaguchi, Ya. M. Blanter, and H. S. J. van der Zant, Phys. Rev. Lett. **105**, 207203 (2010).
[29] D. H. Santamore, A. C. Doherty, and M. C. Cross, Phys. Rev. B **70**, 144301 (2004).
[30] E. A. Laird, F. Pei, W. Tang, G. A. Steele, and L. P. Kouwenhoven, Nano Lett. **12**, 193 (2012).
[31] J.-P. Cleuziou, W. Wernsdorfer, V. Bouchiat, T. Ondarcuhu, and M. Monthioux, Nat. Nanotechnol. **1**, 53 (2006).
[32] B. H. Schneider, S. Etaki, H. S. J. van der Zant, and G. A. Steele, Sci. Rep. **2**, 599 (2012).
[33] See, e.g., C. D. Tesche and J. Clarke, J. Low Temp. Phys. **29**, 301 (1977).
[34] See, e.g., Yu. V. Nazarov and Ya. M. Blanter, *Quantum Transport—Introduction to Nanoscience* (Cambridge University Press, Cambridge, England, 2009).
[35] D. Lee, M. Underwood, D. Mason, A. B. Shkarin, S. W. Hoch, and J. G. E. Harris, Nat. Commun. **6**, 6232 (2015).